Parametric 3D elastic solutions of beams involved in frame structures

Felipe Bordeu[1], Chady Ghnatios[1], Daniel Boulze[2], Beatrice Carles[2],
Damien Sireude[2], Adrien Leygue[1] and Francisco Chinesta[*1]

[1]*GeM UMR CNRS-Centrale Nantes, 1 rue de la Noe, F-44300 Nantes, France*
[2]*AEROLIA, 13 rue Marie-Louise Dissard, BP 73216, 31027 Toulouse, Cedex 3, France*

Abstract. Frame structures have been traditionally represented as an assembling of components, these last described within the beam theory framework. In the case of frames involving complex components in which classical beam theory could fail, 3D descriptions seem the only valid route for performing accurate enough analyses. In this work we propose a framework for frame structure analyses that proceeds by assembling the condensed parametric rigidity matrices associated with the elementary beams composing the beams involved in the frame structure. This approach allows a macroscopic analysis in which only the condensed degrees of freedom at the elementary beams interfaces are considered, while fine 3D parametric descriptions are retained for local analyses.

Keywords: PGD; parametric solutions; model reduction; frame structures; shape optimization

1. Introduction

Frame structures are composed of structural components fastened together. They are very common in nature and thus they inspired engineers that used many variants from the very beginning of structural mechanics. Many times they are assembled in complex structural systems that also involve plates and shells, as usually encountered in aircraft fuselages, as the one depicted in Fig. 1.

In general the design of such structures requires the calculation of stresses, strains and displacements for the design loads. The so-called constitutive law relates strains and stresses. The simplest one consists in linear elasticity. Despite its simplicity many structures are designed for working precisely within the elastic domain. Other designs require considering more complex behaviors not addressed in the present work.

Design problems always involve the solution of a set of partial differential equations in the domains of interest, these ones ranging from beams, columns, plate or shells, to complex assembling of them, with appropriate initial and boundary conditions. The structural elements involved in such mechanical models are degenerated because at least one of its characteristic dimensions is much lower that the other ones. We will understand the consequences of such

∗Corresponding author, Ph.D., E-mail: Francisco.Chinesta@ec-nantes.fr
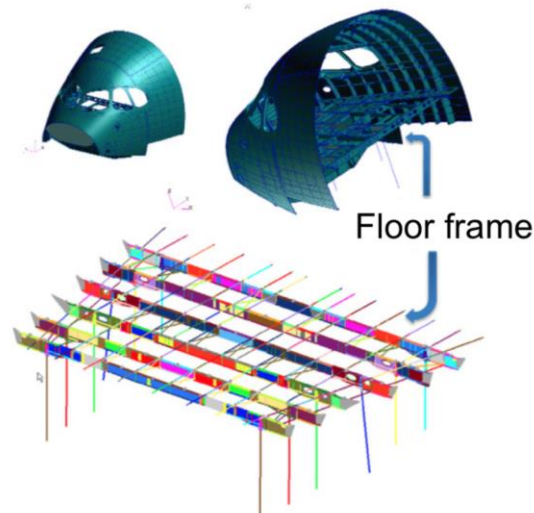
Felipe Bordeu et al.

Fig. 1 Floor-frame structure of an aircraft fuselage. When considering Nastran in the analysis, beams are composed 2D elements where colors identify regions with identical properties. The horizontal lines are 1D elements representing the rails on which seats are located. The vertical lines are 1D elements representing struts stabilizing floor under pressure. In our case we consider these data coming from Nastran but we are performing a 3D elastic analysis using a radically different computational strategy

degeneracy later. When analytical solutions are neither available nor possible because the geometrical or behavior complexities, the solution must be calculated by using any of the available numerical techniques.

Within the numerical framework the solution will be only obtained in a discrete number of points, usually called nodes, distributed in the domain. The solution at those points can be interpolated at any other point in the domain. In general regular nodal distributions are preferred because they offer the best accuracy. In the case of degenerated structural elements one could expect that if the solution evolves significantly in the smallest directions, a large enough number of nodes must be distributed along these dimensions to ensure the accurate representation of the field evolution. In that case, a regular nodal distribution in the whole domain will imply the use of an extremely large number of nodes with the consequent impact on the numerical solution efficiency.

When simple behaviors and domains are addressed semi-analytical models could be considered (see Timoshenko 1955, Timoshenko and Woinowsky-Krieger 1959). For addressing more complex scenarios plate and shell theories were developed allowing, through the introduction of some hypotheses, reducing the 3D complexity to the 2D related to the problem now formulated by considering the in-plane coordinates. There are thousand of papers concerning the proposal and application of plate and shell models (the interested reader can refer to the recent reviews - see Zhang and Yang 2009, Quatu 2012, and the numerous references therein -). Some models are based on the introduction of kinematic hypotheses in the thickness (see Reddy and Arciniega, 2004, among many others). Transverse shear can be also taken into account as described in Viola *et al.* (2013). Recent zig-zag representations (Carrera 2003, Sedira *et al.* 2012), layer-wise models (Kratzig and Jun 2002, Carrera 2002, 2003) and solid-shell approaches (Trinh *et al.* 2011, Naceur

et al. 2013) allow addressing accurately more complex scenarios, by increasing the computational complexity slightly. Stiffeners require an appropriate coupling of beam and shell models in order to perform calculations at a moderate computational cost (Quatmann *et al*. 2013).

When considering beams and assembling of them, strength of materials (Timoshenko 1955, Timoshenko and Young 1982) leads to 1D models. The use of these theories has been extended gradually for addressing larger and more complex geometries and behaviors. However, as soon as richer physics are involved in the models and the considered geometries differ of those ensuring the validity of the different reduction hypotheses, efficient simulations are compromised. In these circumstances as just indicated the reduction from the 3D model to a 2D or 1D simplified one is not obvious, and 3D simulations appear many times as the only valid route for addressing such models, that despite the fact of being defined in degenerated geometries (beam, plate or shell) they seem requiring fully 3D solutions. However in order to integrate such calculations (fully 3D and implying an impressive number of degrees of freedom) in usual design procedures, a new efficient (fast and accurate) solution procedure is urgently needed.

Historically, the Saint-Venant's principle was extensively used in the Ladeveze's works for defining elegant and efficient 3D simplified models (Hochard *et al*. 1993). This technique was then generalized to dynamics (Ladeveze *et al*. 2001) and it allowed a significant reduction of the computational complexity.

Later, a new discretization technique based on the use of separated representations was proposed for addressing space-time nonlinear models by Ladeveze (1999) and then it was generalized for defining general separated representations of solutions involving conformational coordinates (Ammar *et al*. 2006), space and time, and even parameters were considered as extra-coordinates. This technique was called Proper Generalized Decomposition – PGD-. The interested reader can refer to the recent reviews (Chinesta *et al*. 2010, Ammar *et al*. 2011, Ladeveze and Cueto 2011, Chinesta *et al*. 2013, and the primer Chinesta *et al*. 2014) and the references therein. A direct consequence was the separated representations involving the space coordinates. Thus in plate domains an in-plane-out-of-plane decomposition was proposed for solving flow problems in laminates (Ghnatios *et al*. 2015), then for solving thermal problems in extruded geometries (Leygue *et al*. 2013), elasticity problems in plate (Bognet *et al*. 2012) and shell (Bognet *et al*. 2014) geometries and coupled multiphysics problems (Chinesta *et al*. 2012). In these cases the 3D solution was obtained from the solution of a sequence of lower dimensional problems. Refined models considering higher order approximations were considered in Vidal *et al*. (2013).

It is important emphasizing the fact that these approaches are radically different to standard beam, plate and shell approaches. In fact, we propose a 3D solver able to compute the different unknown fields without the necessity of introducing any hypothesis. The most outstanding advantage is that 3D solutions can be obtained with a computational cost characteristic of standard 2D or 1D solutions.

Another appealing feature of separated representations is that it allows circumventing the curse of dimensionality, that is, the solution of a model defined in a high dimensional space of dimension D>3 can be obtained from the solution of a sequence of problems defined in spaces of moderate dimensions (1D, 2D or 3D). For instance, parameters in a model (material parameters, geometrical parameters or boundary conditions) can be set as additional extra-coordinates of the model. In a PGD framework, the resulting model is solved once for life, in order to obtain a general solution that includes all the solutions for every possible value of the parameters, that is, a sort of *computational vademecum*. Under this rationale, optimization of complex problems, uncertainty quantification, simulation-based control and real-time simulation are now at hand,

even in highly complex scenarios, by combining an off-line stage in which the general PGD solution, the vademecum, is computed, and an on-line phase in which, even on deployed, handheld, platforms such as smartphones or tablets, real-time response is obtained as a result of our queries (Chinesta *et al*. 2013, 2014).

In this work we are considering the efficient solution of frame structures composed of complex beams. Different hypotheses will be considered: elastic behavior, small strains and displacements and static regime. Each beam involved in the structural frame is composed of elementary beams (we will consider only four I-beam typologies) that are assembled for composing the complex beams that are also assembled in the frame structure as depicted in Fig. 1.

The optimization of such a structure concerns the shape optimization of each elementary beam involved in each beam composing the frame structure. The three design variables related to each elementary I-beam are the thickness of the web and of the lower and upper flanges, under the constraints of constant beam width and height. Thus, the total number of parameters involved in the optimization of the whole frame structure depicted in Fig. 1 is of 148, number that defines the dimension of the design space.

We can notice immediately that the exploration of the whole design space is impossible when considering standard solution procedures. If we consider that each one of these 148 parameters can take 10 possible values, the number of possible configurations in the design space is 10^{148}, even if such a detailed exploration is not compulsory for performing efficient optimizations.

Frame structure optimization aims reducing the structure weight as much as possible while ensuring many other optimization constraints related to the maximum deflection of each beam, the maximum Von Mises stress and many geometrical constrains, while considering many loading hypotheses. Because some elementary I-beams involve circular and elliptical holes and they could in future works include other local complexities, we decided to perform a fully 3D elastic analysis of them. Moreover, results of fully 3D analyses could be also used for validating simplified approaches based on considering beam solutions coming from strength of materials or theory of structures, or the ones based on considering each elementary I-beam as an assemblage of three plates related to its web and both flanges.

The main difficulty when addressing the structural optimization process is the necessity of evaluating the global elastic solution for each trial structure considered within the design space. With 148 design parameters and tens of constraints, robust and powerful optimization strategies will be needed, because one could expect thousands of 3D elastic solutions related to the trial structures.

In order to alleviate the cost of optimization processes of such kind of frame structures we propose in this paper the construction of 4 computational vademecums, one for each elementary I-beam typology, containing the parametric 3D elastic solution for given displacements at both ends. We discuss the choice of such displacements later. Then these vademecums will be assembled for composing the different beams involved in the frame structure. Then, all them will be assembled with the condensed fuselage structure (in the application here considered) from the degrees of freedom related to the beams ends. Thus, it results finally a sort of parametric frame structure model whose solution, as soon as the parameters are chosen, only requires the solution of a linear system of few hundreds of equations, despite the millions of degrees of freedom involved in the different fields approximation.

The main numerical ingredients considered in the present work concern: (i) the space separated representation for the high fidelity solution of the 3D linear elastic and static problems at the level of each elementary I-beam; (ii) the introduction of four beam parameters as extra-coordinates of

the elastic problem related to each elementary I-beam: its length and the beam web and flanges thickness; and (iii) the assembling of the resulting parametric solutions for defining the beams and then the whole frame structure.

In what follows we revisit in section 2 the main numerical techniques involved in the previous items. In section 3 we describe the construction of the elementary I-beams parametric solutions that will be assembled to define the frame structure in section 4. Finally numerical results will be addressed and discussed in section 5.

2. Numerical techniques

In this section we revisit separated representations involving an in-plane-out-of-plane separated representation. Then geometrical parameters will be introduced as model extra-coordinates in order to define a powerful shape optimization framework.

2.1 In-plane-out-of-plane separated representation

In many applications, the computational domain can be expressed as a product of lower dimensional domains. For example a hexahedral domain can be written as $\Omega = \Omega_x \times \Omega_y \times \Omega_z$, an extruded domain as $\Omega = \Omega_{xy} \times \Omega_z$ where Ω_{xy} represents the usually geometrically complex cross section and Ω_z the extrusion axis. Plates can also be written in the form $\Omega = \Omega_{xy} \times \Omega_z$ where in this case Ω_{xy} represents the middle surface and Ω_z the plate thickness.

Thus, a scalar field $u(x,y,z)$ could be approximated in the separated form

$$u(x,y,z) \approx \sum_{i=1}^{N} P_i(x,y) \cdot T_i(z) \tag{1}$$

where the 3D solution only requires the calculation of about N 2D-functions $P_i(x,y)$ and N one-dimensional functions $T_i(z)$, the computational cost associated to the last being negligible compared with the computational cost related to the computation of the two-dimensional functions. We discuss later the details related to the calculation of both kind of functions, deeply described in Chinesta *et al*. (2014).

When we consider a vector unknown field, as the one related to the elastic displacements, $\mathbf{u}(x,y,z)$, the separated approximation (1) is considered for each of its components, i.e.

$$u_j(x,y,z) \approx \sum_{i=1}^{N} P_i^j(x,y) \cdot T_i^j(z) \tag{2}$$

The compact form of Eq. (2) writes making use of the Hadamard product

$$\mathbf{u}(x,y,z) \approx \sum_{i=1}^{N} \mathbf{P}_i(x,y) \circ \mathbf{T}_i(z) \tag{3}$$

where vectors $\mathbf{P}_i$ and $\mathbf{T}_i$ contains functions P_i^j and T_i^j respectively. Because neither the number of terms N in the separated representation of the displacement field nor the dependence on z of functions T_i^j are assumed *a priori*, the approximation is flexible enough for representing the fully 3D solution, being obviously more general than theories assuming particular, *a priori,*

evolutions in the thickness direction *z*.

Remark. The use of separated representations (1) or (3) is quite general. When the solution is regular enough it can be separated as a finite sum involving few terms (*N*). When it is badly separable the number of terms increases too much and in that case its use does not offer major interest. In general, to be efficient, the separated representation requires the separated representation of the domain itself. In the case of a cube, the three space coordinates can be easily separated. In the case of plates the most natural separation concerns the in-plane and the out-of-plane coordinates. In the case of a rod, the most natural separated representation concerns the coordinates related to the cross section and the one related to the rod axis. When considering assembled structures we can separate each component and then assembling all them by using any domain decomposition strategy as for example the one considered in Nazeer *et al.* (2014).

Let's consider a linear elasticity problem on a plate domain $\Omega=\Omega_{xy}\times\Omega_z$. The weak formulation reads

$$\int_{\Omega} \varepsilon^{*T} \cdot \mathbf{K} \cdot \varepsilon \, \mathrm{d}\mathbf{x} = \int_{\Omega} \mathbf{u}^{*T} \cdot \mathbf{f} \, \mathrm{d}\mathbf{x} + \int_{\Gamma_N} \mathbf{u}^{*T} \cdot \mathbf{F} \, \mathrm{d}\mathbf{x} \tag{4}$$

where $\mathbf{K}$ is the generalized 6×6 Hooke tensor, $\mathbf{f}$ represents the volumetric body forces while $\mathbf{F}$ represents the traction applied on the boundary Γ_N. The separation of variables previously introduced yields the following expression for the derivatives of the displacement components:

$$\begin{cases} u_{j,k}(x,y,z) \approx \sum_{i=1}^{N} P_{i,k}^{j}(x,y) \cdot T_i^j(z), & k = x,y \\[2mm] u_{j,k}(x,y,z) \approx \sum_{i=1}^{N} P_i^{j}(x,y) \cdot T_{i,k}^j(z), & k = z \end{cases} \tag{5}$$

that allows writing the vector form of the strain tensor ε in Eq. (4) in a separated form (see Bognet *et al.* 2012, for additional details).

The separated representation constructor proceeds by computing a term of the sum (3) at each iteration. Assuming that the first *n*−1 modes (terms of the finite sum) of the solution were already computed, the solution enrichment reads

$$\mathbf{u}^n(x,y,z) = \mathbf{u}^{n-1}(x,y,z) + \mathbf{P}_n(x,y)\mathbf{o}\mathbf{T}_n(z) \tag{6}$$

where functions $\mathbf{P}_n(x,y)$ and $\mathbf{T}_n(z)$ are unknown at the present iteration. The test function $\mathbf{u}^*$, within the Galerkin framework, reads

$$\mathbf{u}^*(x,y,z) = \mathbf{P}^*(x,y)\mathbf{o}\mathbf{T}_n(z) + \mathbf{P}_n(x,y)\mathbf{o}\mathbf{T}^*(z) \tag{7}$$

The introduction of Eqs. (6) and (7) into (4) results in a non-linear problem. We proceed by considering the simplest linearization strategy, an alternated directions fixed point algorithm that proceeds by calculating $\mathbf{P}_n^m$ from $\mathbf{T}_n^{m-1}$ (*m* refers to the nonlinear iteration) and then by updating $\mathbf{T}_n^m$ from the just calculated $\mathbf{P}_n^m$. The iteration procedure continues until convergence, that is, until reaching the fixed point $\left\| \mathbf{P}_n^m(x,y)\mathbf{o}\mathbf{T}_n^m(z) - \mathbf{P}_n^{m-1}(x,y)\mathbf{o}\mathbf{T}_n^{m-1}(z) \right\| \leq \varepsilon$. After convergence we make the assignments $\mathbf{P}_n^m \rightarrow \mathbf{P}_n$ and $\mathbf{T}_n^m \rightarrow \mathbf{T}_n$. The enrichment stops when the model residual becomes small enough. Other error indicators are available (Ammar *et al.* 2010)

When $\mathbf{T}_n$ is assumed known (we omit the superscript $m-1$ related to the nonlinear loop for notational simplicity), we consider the test function $\mathbf{u}^*(x,y,z)=\mathbf{P}^*(x,y)\text{o}\mathbf{T}_n(z)$. By introducing the trial and test functions into the weak form and then integrating in Ω_z because all the functions depending on the thickness coordinate are known, we obtain a 2D weak formulation defined in Ω_{xy} whose discretization (by using a standard discretization strategy, e.g., finite elements) allows computing $\mathbf{P}_n$ (again we omit the superscript m related to the nonlinear loop for notational simplicity).

Analogously, when $\mathbf{P}_n$ is assumed known, the test function reads $\mathbf{u}^*(x,y,z)=\mathbf{P}_n(x,y)\text{o}\mathbf{T}^*(z)$. By introducing the trial and test functions into the weak form and then integrating in Ω_{xy} because all the functions depending on the in-plane coordinates (x,y) are at present known, we obtain a 1D weak formulation defined in Ω_z whose discretization (using any technique for solving standard ODE equations) allows computing $\mathbf{T}_n$.

As discussed in Bognet *et al*. (2012) this separated representation allows computing 3D solutions while keeping a computational complexity characteristic of 2D solution procedures. If we consider a hexahedral domain discretized using a regular structured grid with M_x, M_y and M_z nodes in the x, y and z directions respectively, usual mesh-based discretization strategies imply a challenging issue because the number of nodes involved in the model scales with $M_x \cdot M_y \cdot M_z$, however, by using the separated representation and assuming that the solution involves N modes, one must solve about N 2D problems related to the functions involving the in-plane coordinates and the same number of 1D problems related to the functions involving the thickness coordinate. The computing time related to the solution of the one-dimensional problems can be neglected with respect to the one required for solving the two-dimensional ones. Thus, the resulting complexity scales as $N \cdot M_x \cdot M_y$. By comparing both complexities we can notice that as soon as $M_z > N$ the use of separated representations leads to impressive computing time savings, making possible the solution of models never until now solved, and even using light computing platforms, as depicted in Fig. 4 in Bognet *et al*. (2012).

2.2 Parametric solutions involving the computational domain

The parameters defining the computational domain can be considered as extra-coordinates within the PGD framework. This allows us to compute a general parametric solution for any computational domain defined from the chosen geometrical parameters, these taking values in their respective domains. A detailed description on this feature was addressed in Chinesta *et al*. (2013) and Chinesta *et al*. (2014). The idea behind it is quite simple. Imagine a simple one-dimensional differential operator $\dfrac{du}{dx}$ with $x \in \Omega_x = (0, L)$ and that we are interested in calculating the solution $u(x)$ in different domains characterized by their length $L \in \Lambda$. Now it suffices considering the change of variable $x = \lambda \cdot L$, $\lambda \in (0,1)$, that results in

$$\frac{du}{dx} = \frac{du}{d\lambda} \cdot \frac{d\lambda}{dx} = \frac{du}{d\lambda} \cdot \frac{1}{L} \tag{8}$$

that allows looking for $u(\lambda, L)$ with $\lambda \in (0,1)$ and $L \in \Lambda$, in the separated form

$$u(\lambda, L) \approx \sum_{i=1}^{N} \Upsilon_i(\lambda) \cdot \Psi_i(L) \tag{9}$$
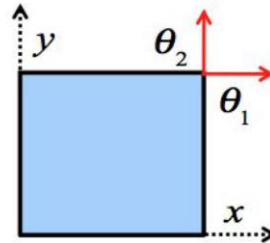
Fig. 2 Parametric domain

This procedure can be generalized to vector fields, multidimensional spaces and many geometrical parameters, as described in Chinesta *et al*. (2013) and considered in Ammar *et al*. (2014).

2.2 Towards efficient shape optimization

In general shape optimization implies the definition of a cost function and the search of the optimum parameters (e.g., geometrical parameters describing the family of possible shapes) defining the minimum of that cost function. The process starts by choosing a tentative set of parameters. Then, the process is simulated by discretizing the equations defining the problem in the geometry defined by the tentative geometrical parameters. This solution is the most costly step of the optimization procedure. As soon as that solution is available, the cost function can be evaluated and its optimality checked. If the chosen parameters do not define a minimum of the cost function, the parameters should be updated and the solution recomputed. The procedure continues until reaching an acceptable minimum of that cost function.

To illustrate the proposed procedure that we will use in what follows, we consider a model defined in the domain sketched in Fig. 2, whose parametric space reduces to the horizontal and vertical displacement of the upper right corner, θ_1 and θ_2, we could summarize traditional optimization procedures as follows:

Until reaching a minimum of the cost function $C(\theta_1, \theta_2)$ proceed by:

1. Computing the unknown field related to the trial choice of the geometry, i.e. $u(\xi, \eta; \theta_1, \theta_2)$ (here (ξ, η) are the coordinates associated to the reference square)

2. Computing the cost function $C(\theta_1, \theta_2)$ from the just calculated model solution.

3. Optimality checking. While the optimum is not reached, update the geometry, by using an appropriate strategy, and come back to step 1.

In the approach proposed in Ammar *et al*. (2014) and considered in the present work the procedure is substantially different. It proceeds as follows:

• Compute the unknown field in any possible geometry, i.e., $u(\xi, \eta, \theta_1, \theta_2)$ (here the location of the upper-right corner play the same role that the space coordinates), the problem becoming multidimensional and then it will be solved by using the PGD separated representation.

• Until reaching a minimum of the cost function $C(\theta_1, \theta_2)$ proceed by:

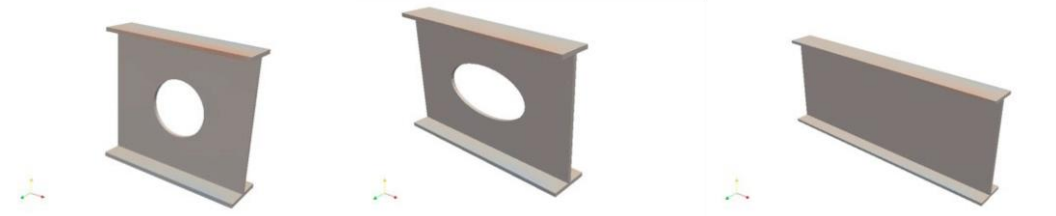1. Particularizing the parametric solution to the considered values of the geometrical parameters.

Fig. 3 Elementary I-beams involved in the larger beams constituting the frame

2. Computing the associated cost function $C(\theta_1, \theta_2)$.

3. Optimality checking. While the optimum is not reached, update the geometry by using an appropriate strategy and come back to step 1.

Thus, by using this approach the model is solved only once and then it is particularized for any choice of the geometry. The price to pay is the necessity of solving a multidimensional model that now has as coordinates the space and all the geometrical parameters. The separated representation of the parametric solution writes

$$u(\xi, \eta, \theta_1, \theta_2) = \sum_{i=1}^{N} X_i(\xi, \eta) \cdot F_i(\theta_1) \cdot G_i(\theta_2) \tag{10}$$

To build up such separated representation we must compute the functions defined in the space domain and the one-dimensional functions related to both geometrical parameters now assumed as model extra-coordinates.

3. Elementary I-beams parametric solutions

We consider the different typologies of the elementary I-beams involved in the frame structure depicted in Fig. 1, three of them illustrated in Fig. 3, the fourth one being similar to the one involving a circular hole, but containing a circular hole of larger diameter.

As these four elementary beams are assembled into the frame beams depicted in Fig. 1 by considering different length of them we decided to include the elementary beams length as a model coordinate. In the same way, as we are interested in reducing as much as possible the different elementary beams web and flanges thickness in order to optimize the frame structure, we will consider these three thickness as extra-coordinates.

Thus each elementary I-beam model consists of a 3D elastic solution for any length l and any thickness of the beam web and the upper and lower flanges, ω, f and g respectively. Thus the displacement, defined in a space of dimension 7, could be written as

$$\mathbf{u}^k(\mathbf{X}, l, \omega, f, g) \approx \sum_{i=1}^{N} \mathbf{R}_i^k(\mathbf{X}) \circ \mathbf{S}_i^k(l) \circ \mathbf{W}_i^k(\omega) \circ \mathbf{F}_i^k(f) \circ \mathbf{G}_i^k(g) \tag{11}$$

where the superscript $k(k=1,2,3,4)$ refers to the elementary I-beam considered. The different coordinates are defined in theirs respective intervals: $\mathbf{X} \in \Omega^r$, $l \in \Omega_l$, $\omega \in \Omega_\omega$, $f \in \Omega_f$ and $g \in \Omega_g$.

A mapping transforms the reference domain Ω^r into the real one Ω, the last of length l and web, upper and lower flanges thickness, ω, f and g respectively. Points in the reference domain Ω^r are
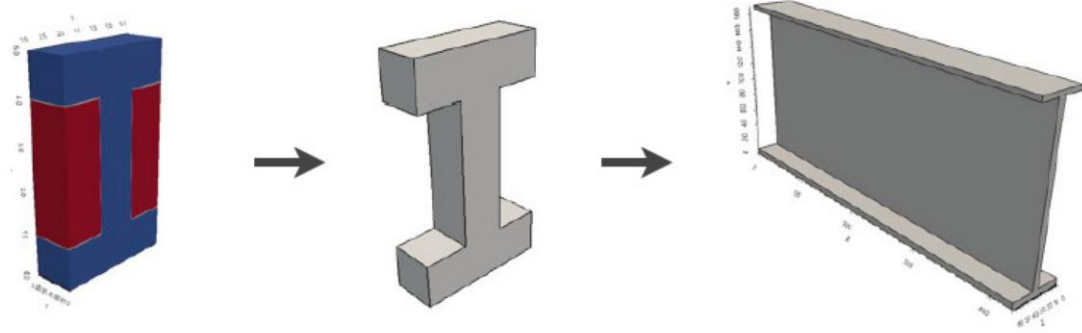
Fig. 4 Sketch of the mapping of the parametric domain into real elementary I-beam

denoted by **X** whereas the ones in the real elementary beam Ω are denoted by **x**. The mapping $\Omega^r \rightarrow \Omega$ is illustrated in Fig. 4.

The previous separated representation (11) requires the solution of several 3D problems for calculating space functions $\mathbf{R}_i^k(\mathbf{X})$. For alleviating the associated computational cost we can proceed to a further separation, the one allowing to perform an in-plane-out-of plane separated representation, the in-plane being the beam axis X and height Y and the out-of-plane being the beam width Z. The most natural choice in the case of profiles considers the in-plane coordinates the ones related to the profile cross section (Y, Z) and the out-of-plane the one related to the beam axis X, however such a decomposition does not allows describing profiles containing holes that cannot be represented in such separated form. Thus, the separated representation of the parametric displacement writes

$$\mathbf{u}^k(X,Y,Z,l,\omega,f,g) \approx \sum_{i=1}^{N} \mathbf{P}_i^k(X,Y) \circ \mathbf{T}_i^k(Z) \circ \mathbf{S}_i^k(l) \circ \mathbf{W}_i^k(\omega) \circ \mathbf{F}_i^k(f) \circ \mathbf{G}_i^k(g) \qquad (12)$$

whose complexity reduces from the 3D characteristic of formulation (11) to the 2D associated with Eq. (12) whose construction only requires the solution of a series of 2D problems related to the calculation of functions $\mathbf{P}_i^k(X,Y)$ (being the cost associated with all the other 1D solutions negligible).

In order to compute the parametric elastic solution of each one of the four elementary I-beams, we must prescribe appropriate loadings (forces or displacements). First, we considered the off-line elastic solution associated with different loadings applied on the whole beams (each one composed of several elementary I-beams with different choices of the web and flanges thickness). From these solutions (computationally expensive but off-line) we verified the fact that the displacement field at the elementary I-beam interfaces can be fully described by the usual beam theory kinematic torsor composed of three unit displacement and three unit rotations $\aleph = (\delta_x, \delta_y, \delta_z, \vartheta_x, \vartheta_y, \vartheta_z)$. We can then conclude that the 3D effects are mostly located inside the elementary I-beams but that they do not reach (significantly) the elementary I-beam ends.

Remark. All the external forces applied on the frame structure are assumed acting at the I-beam interfaces. When it is not the case two simple alternatives exist: (i) move the loads to the neighbor interfaces or (ii) consider the load location on the beam as an extra-coordinate as described in Niroomandi *et al.* (2013).

Remark. In fact the kinematics at the interface between two consecutive I-beams can be expressed from a few number of modes (in general lower than the 6 elementary displacements/rotations involved in the kinematic torsor $\aleph$) that can be extracted by applying a singular value decomposition to the off-line solutions obtained by considering different loadings and elementary I-beams web and flanges thickness. However, in that case the reduced basis at each interface, even if smaller than the one involved in $\aleph$, results different at each interface between two consecutive elementary I-beams. For this reason in what follows we consider the reduced basis expressed by the standard kinematic torsor $\aleph$. When the complexity of the considered systems avoids the use of such standard torsor the simplest choice consists of assuming a common basis integrating the significant modes at each interface. Even if the resulting number of modes could increase significantly, it will remain moderate.

Now, because the linearity of the problem, we can compute the parametric elastic solution for each elementary I-beam by prescribing at each beam end the displacement field associated with one of the elements of the kinematic torsor, all the others being zero.

Thus, we obtain 12 parametric elastic solutions for each one of the four elementary I-beams: $\mathbf{u}_m^{k+}(X,Y,Z,l,\omega,f,g)$ and $\mathbf{u}_m^{k-}(X,Y,Z,l,\omega,f,g)$ with $k=1,...,4$ and $m=1,...,6$. In these expressions the superscript k refers to each I-beam typology, the superscript $(+)$ and $(-)$ refer respectively to I-beam right and left ends and the index m refers to the active element of the kinematic torsor considered in the elastic parametric solution.

Due to the model linearity, any possible parametric solution in each I-beam can be written as a linear combination of these 12 solutions, that is:

$$\mathbf{u}^k(X,Y,Z,l,\omega,f,g) = \sum_{m=1}^{6} \gamma_m^+ \mathbf{u}_m^{k+}(X,Y,Z,l,\omega,f,g) + \sum_{m=1}^{6} \gamma_m^- \mathbf{u}_m^{k-}(X,Y,Z,l,\omega,f,g) \quad (13)$$

Knowing the parametric displacement fields $\mathbf{u}_m^{k+}(X,Y,Z,l,\omega,f,g)$ and $\mathbf{u}_m^{k-}(X,Y,Z,l,\omega,f,g)$ we can compute the parametric stress fields everywhere by calculating the parametric strain and then applying the linear elastic behavior law. The integration of the stresses on the elementary I-beam ends allows computing the three resultant forces and moments at both ends of each elementary I-beam, i.e., the mechanical torsor. The mechanical torsor $\Im$ is composed of three forces and three moments $\Im = (\mathbf{F}_x, \mathbf{F}_y, \mathbf{F}_z, \mathbf{M}_x, \mathbf{M}_y, \mathbf{M}_z)$.

4. Parametric frame structure

From the previous developments we can define the elementary I-beam condensed parametric rigidity matrix relating the kinematic and mechanical torsors at the I-beam ends.

Thus we can write for each elementary I-beam n ($n=1,...,4$)

$$\begin{pmatrix} \Im^{n-} \\ \Im^{n+} \end{pmatrix} = \begin{pmatrix} \mathbf{K}^{n--} & \mathbf{K}^{n-+} \\ \mathbf{K}^{n+-} & \mathbf{K}^{n++} \end{pmatrix} \begin{pmatrix} \mathbf{U}^{n-} \\ \mathbf{U}^{n+} \end{pmatrix} \quad (14)$$

that represents a parametric elastic beam. In expression (14) vectors $\mathbf{U}^{n-}$ and $\mathbf{U}^{n+}$ contains coefficients γ_m^- and γ_m^+ involved in Eq. (13).

A soon as the geometrical parameters (l,ω,f,g) are chosen, the condensed parametric rigidity

matrix results in the beam rigidity matrix. For uniform beams this matrix coincides with the standard and well-known beam rigidity matrix.

Now, the assembling proceeds as in standard structural analysis by writing the forces and moments equilibrium at each I-beam interfaces. Assuming the external forces and moments applying in each interface s ($s=1,...,S$) given by $\mathfrak{I}^s$, it results after assembling all the elementary I-beams composing the frame beams

$$\mathbf{K} \cdot \mathbf{U} = \mathbf{F} \tag{15}$$

where $\mathbf{U}^T=(\mathbf{U}^1,...,\mathbf{U}^S)$ and $\mathbf{F}^T=(\mathbf{F}^1,...,\mathbf{F}^S)$.

The resulting algebraic linear system contains 6 degrees of freedom at each interface, that results in general in a linear systems involving few hundreds of degrees of freedom despite the high fidelity description (equivalent to thousands of millions degrees of freedom) considered for representing each parametric 3D I-beam solution.

As soon as the kinematic torsor is available at each interface, the 3D representations of displacements, strains and stresses can be calculated at each point of each elementary I-beam involved in the beams composing the frame structure. This calculation can be performed efficiently (accurate and fast) because all the information is available in the parametric solution related to each elementary I-beam.

5. Results and discussion

By applying the procedure just described we can compose any beam of the frame structure by assembling different elementary I-beam typologies, by fixing their different length and web and flanges thickness. If the structure frame involves other elementary typologies, 12 parametric solutions should be pre-computed in order to define the elementary beam condensed parametric rigidity matrix.

When focusing in the problem depicted in Fig. 1, each one of the six beams is composed of several elementary I-beams of different lengths. When fixing the 148 thickness defining the design variables (web and flanges thickness of each elementary I-beam) and enforcing the external loading, we can proceed to the assemblage and solution of the resultant condensed structure at the interfaces. The solution allows computing the displacement everywhere.

The considered algorithm consists of:

• Compose each beam of the frame by considering elementary beams, like in a "lego", of 4 different typologies. If new typologies are required, 12 parametric problems must be solved, as previously described, to define the parametric stiffness matrix of each new elementary beam typology.

• As soon as the length and thickness of each elementary beam are specified the parametric stiffness matrix of each beam is particularized and then all them assembled into the frame stiffness matrix that is then assembled with the condensed matrix of the fuselage. The vector containing the forces applying at the elementary beam interfaces is also constructed.

• The linear algebraic system is then solved to obtained the generalized displacements and forces at the elementary beam interfaces from which they can be extended everywhere.

• Different quantities of interest are then evaluated and the optimality and restrictions checked. If both criteria are not satisfied webs and flanges thickness are updated and then the frame is assembled and solved again. The process continues until fulfilling optimality criteria while
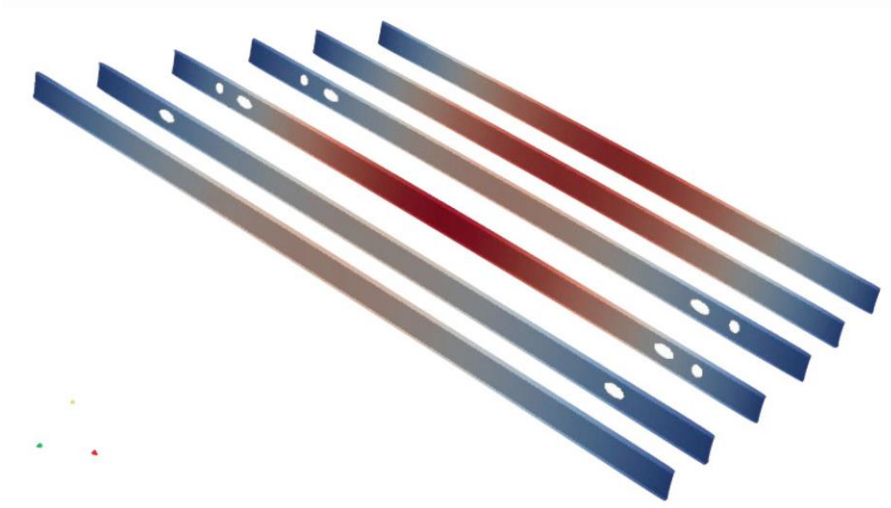
Fig. 5 Frame structure displacement field for a particular choice of the loading and the geometrical parameters (web and flanges thickness of each elementary I-beam)

satisfying all the kinematical (maximum displacements) and mechanical (maximum Von Mises stress) constraints.

More concretely, the frame illustrated in Fig. 1 and here considered is composed of 6 beams, four of them involving 24 elementary I-beams (of the four typologies previously described) and the remaining two are composed of 22 elementary I-beams. The boundary conditions are not explicitly enforced because these 6 beams are assembled with the condensed fuselage stiffness matrix at their ends. 50 loading cases where analyzed to ensure the structural integrity of the structure and the material properties were the ones corresponding to aluminum.

Four different constraints were checked, concerning (i) the maximal deflection of the beams; (ii) the maximum bending moment transmitted to ten fuselage at the six beam ends; (iii) the gap in the web and flanges thickness from one elementary beam to the neighboring ones, and (iv) the maximum Von Mises stress. These constraints were checked at each step of the optimization algorithm.

A solution associated to a particular choice of external loads and design parameters is depicted in Fig. 5. This solution is in perfect agreement with the one obtained by using any well-experienced commercial simulation code, whose solution was too expensive from the computational point of view to be considered in optimization processes where too many calculations could be required. Here 3D solutions for some geometries by using commercial software where considered in the verification of the I-beams parametric solutions and for validation the whole structural analysis.

In order to conclude on the performances of the strategy just presented, and that was fully verified, we are given some indications on the complexity of the different steps.

• The description of the different elementary I-beams (four in the present application) is equivalent to the use of 40.000 nodes in Ω^r and 10^8 in the parametric domain (involving four dimension: the length and three thickness coordinates, each one consisting in 100 possible values). Obviously such a richness is excessive in the present application that as discussed previously is quite well represented by standard beam theory, but it serves to emphasize the possibilities of the

proposed strategy that can represent solutions with an unimaginable accuracy.

• Due to the separated representation involved in the PGD solver the complexity of such extremely fine description scales with few thousands of nodes involved in the description of the in-plane functions (the others coordinates involve the solution of 1D problems whose complexity can be neglected). The calculation and post compression of the resulting separated representation of the parametric elastic solution in each elementary I-beam represents less than one-day computation in an ordinary laptop. This task is performed only once for each elementary I-beam typology in order to extract its parametric solution.

• When fixing a loading and the web and flanges thickness of each elementary beam, the assemblage of the global structure needs about 0.3 seconds in an ordinary laptop. The solution of the assembled linear system needs less than 0.5 second. Then the evaluation time of a particular configuration (frame structure) is performed in less than 1 second. This time is characteristic of standard structural analysis, however here we are considering rigidity matrices that takes into account eventual 3D effects and we are post-processing 3D solutions.

• The post-processing time could be greater, mainly if one must determine the maximum Von Mises stress in each elementary I-beam. In that case if we look for the stress at each node (about 40.000) in each one of the hundreds elementary I-beams composing the whole frame, the computing time results of few tens of second. Obviously when using the available information coming from the beam theory that applies quite well in the present case, the computing time can be reduced to few fractions of second.

• In the general case, with few tens of seconds involved in each evaluation of a trial configuration, the computing time involved in the optimization involving 148 design variables and hundreds of constraints, could be prohibitive. When using the information available on the regions in which the maximum stresses locate due to the solution knowledge, efficient optimizations can be envisaged.

• In the general case, the choice of the optimization strategy is a key-point, and constitutes a work in progress. The coupling between our procedure and the use of robust commercial optimization software based on the construction of an intermediate metamodel (e.g., Macros from Datadvance *http://www.datad\-vance.net*) constitutes an appealing route to perform robust optimization based on high fidelity 3D descriptions of frame structures.

6. Conclusions

This work proposes a new methodology for addressing the calculation and optimization of complex frames composed of complex beams. In order to speed as much as possible the calculation without scarifying the solution accuracy and the eventual 3D features (many times existing locally) we propose the construction of different parametric elastic 3D solutions related to the different elementary beams composing the complex beams that integrate the structural frame.

These parametric solutions contain the elastic solution for any geometry (length and web and flanges thickness) and any kinematic torsor acting on the elementary beam-ends. As soon as the beam geometry is defined, the elementary beam condensed matrix are assembled and the resulting linear system solved.

The procedure here proposed allows solving any frame (among a multitude of them, 10^8 in the application here considered) in a laptop while keeping the fully 3D resolution, in some fractions of second. This efficiency allows envisaging the use of the just described procedure for constructing

metamodels that could be used for efficient shape optimization of structural frames. The analysis of this potentiality constitutes a work in progress.

References

Ammar, A., Mokdad, B., Chinesta, F. and Keunings, R. (2006), "A new family of solvers for some classes of multidimensional partial differential equations encountered in kinetic theory modeling of complex fluids", *J. Non-Newton. Fluid Mech.*, **139**, 153-176.

Ammar, A., Chinesta, F., Diez, P. and Huerta, A. (2010), "An error estimator for separated representations of highly multidimensional models", *Comput. Meth. Appl. Mech. Eng.*, **199**, 1872-1880.

Ammar, A. Huerta, A., Chinesta, F., Cueto, E. and Leygue, A. (2014), "Parametric solutions involving geometry: a step towards efficient shape optimization", *Comput. Meth. Appl. Mech. Eng.*, **268**, 178-193.

Bognet, B., Leygue, A., Chinesta, F., Poitou, A. and Bordeu, F. (2012), "Advanced simulation of models defined in plate geometries: 3D solutions with 2D computational complexity", *Comput. Meth. Appl. Mech. Eng.*, **201**, 1-12.

Bognet, B., Leygue, A. and Chinesta, F. (2014), "Separated representations of 3D elastic solutions in shell geometries", *Adv. Model. Simul. Eng. Sci.*, **1**(1), 1-34.

Carrera, E. (2002), "Theories and finite elements for multilayered, anisotropic, composite plates and shells", *Arch. Comput. Meth. Eng.*, **9**(2), 87-140.

Carrera, E. (2003), "Historical review of Zig-Zag theories for multilayered plates and shells", *Appl. Mech. Rev.*, **56**(3), 287.

Carrera, E. (2003), "Theories and finite elements for multilayered plates and shells: A unified compact formulation with numerical assessment and benchmarking", *Arch. Comput. Meth. Eng.*, **10**(3), 215-296.

Chinesta, F., Ammar, A. and Cueto, E. (2010), "Recent advances and new challenges in the use of the Proper Generalized Decomposition for solving multidimensional models", *Arch. Comput. Meth. Eng.*, **17**, 327-350.

Chinesta, F., Ammar, A., Leygue, A. and Keunings, R. (2011), "An overview of the Proper Generalized Decomposition with applications in computational rheology", *J. Non-Newton. Fluid Mech.*, **166**, 578-592.

Chinesta, F., Ladeveze, P. and Cueto, E. (2011), "A short review in model order reduction based on Proper Generalized Decomposition", *Arch. Comput. Meth. Eng.*, **18**, 395-404.

Chinesta, F., Leygue, A., Bognet, B., Ghnatios, Ch., Poulhaon, F., Bordeu, F., Barasinski, A., Poitou, A., Chatel, S. and Maison-Le-Poec, S. (2012), "First steps towards an advanced simulation of composites manufacturing by automated tape placement", *Int. J. Mater. Form.*, **7**(1), 81-92.

Chinesta, F., Leygue, A., Bordeu, F., Aguado, J.V., Cueto, E., Gonzalez, D., Alfaro, I., Ammar, A. and Huerta, A. (2013), "Parametric PGD based computational vademecum for efficient design, optimization and control", *Arch. Comput. Meth. Eng.*, **20**, 31-59.

Chinesta, F., Keunings, R., Leygue, A. (2014), *The Proper Generalized Decomposition for Advanced Numerical Simulations*, A Primer, Springerbriefs, Springer.

Ghnatios, Ch., Chinesta, F. and Binetruy, Ch. (2015), "The squeeze flow of composite laminates", *International Journal of Material Forming*. (in Press)

Hochard, Ch., Ladeveze, P. and Proslier L. (1993), "A simplified analysis of elastic structures", *Eur. J. Mech. A/Solid.*, **12**(4), 509-535.

Kratzig, W.B. and Jun, D. (2002), "Multi-layer multi-director concepts for D-adaptivity in shell theory", *Comput. Struct.*, **80**(9), 719-734.

Ladeveze, P. (1999), *Nonlinear Computational Structural Mechanics - New Approaches and Non-IncrementalMethods of Calculation*, Springer, Berlin.

Ladeveze, P., Arnaud, L., Rouch, P. and Blanz, C. (2001), "The variational theory of complex rays for the calculation of medium-frequency vibrations", *Eng. Comput.,* **18**(1–2), 193-221.

Leygue, A., Chinesta, F., Beringhier, M., Nguyen, T.L., Grandidier, J.C., Pasavento, F. and Schrefler, B.

(2013), "Towards a framework for non-linear thermal models in shell domains", *Int. J. Numer. Meth. Heat Fluid Flow*, **23**, 55-73.

Naceur, H., Shiri, S., Coutellier, D. and Batoz, J.L. (2013), "On the modeling and design of composite multilayered structures using solid-shell finite element model", *Finite Elem. Anal. Des.*, **70**, 1-14.

Nazeer, M., Bordeu, F., Leygue, A. and F. Chinesta, F. (2014), "Arlequin based PGD domain decomposition", *Comput. Mech.*, **54**(5), 1175-1190.

Niroomandi, S., Gonzalez, D., Alfaro, I., Bordeu, F., Leygue, A., Cueto, E. and Chinesta, F. (2013), "Real time simulation of biological soft tissues : A PGD approach", *Int. J. Numer. Meth. Biomed. Eng.*, **29**(5), 586-600.

Qatu, M.S. (2012), "Review of recent literature on static analyses of composite shells: 2000-2010", *Open J. Compos. Mater.*, **2**(3), 61-86.

Reddy, J.N. and Arciniega, R.A. (2004), "Shear deformation plate and shell theories: from Stavsky to present", *Mech. Adv. Mater. Struct.*, **11**(6), 535-582.

Sedira, L., Ayad, R., Sabhi, H., Hecini, M. and Sakami, S. (2012), "An enhanced discrete Mindlin finite element model using a zigzag function", *Euro. J. Comput. Mech.*, **21**(1-2), 122-140.

Timoshenko, S.P. (1955), *Strength of Materials*, Van Nostrand.

Timoshenko, S.P. and Woinowsky-Krieger, S. (1959), *Theory of Plates and Shells*, McGraw-Hill.

Timoshenko, S.P. and Young, D.H. (1982), *Theory of Structures*, McGraw-Hill.

Trinh, V.D., Abed-Meraim, F. and Combescure, A. (2011), "A new assumed strain solid-shell formulation "SHB6" for the six-node prismatic finite element", *J. Mech. Sci. Tech.*, **25**(9), 2345-2364.

Vidal, P., Gallimard, L. and Polit, O. (2013), "Proper generalized decomposition and layer-wise approach for the modeling of composite plate structures", *Int. J. Solid. Struct.*, **50**(14-15), 2239-2250.

Viola, E., Tornabene, F. and Fantuzzi, N. (2013), "Static analysis of completely doubly-curved laminated shells and panels using general higher-order shear deformation theories", *Compos. Struct.*, **101**, 59-93.

Zhang, Y.X. and Yang, C.H. (2009), "Recent developments in finite element analysis for laminated composite plates", *Compos. Struct.*, **88**(1), 147-157.

AB